Controlled leaky wave radiation from anisotropic epsilon near zero metamaterials

Klaus Halterman,[1] Simin Feng,[1] and Viet Cuong Nguyen[2]
[1]*Naval Air Warfare Center, Michelson Laboratory, Physics Division, China Lake, California 93555, USA*
[2]*Photonics Research Centre, School of Electrical and Electronics Engineering, Nanyang Technological University, 50 Nanyang Avenue, Singapore 639798, Singapore*

(Received 7 April 2011; revised manuscript received 21 July 2011; published 18 August 2011)

We investigate the emission of electromagnetic waves from biaxial subwavelength metamaterials. For anisotropic structures that exhibit a vanishing dielectric response along the longitudinal axis and possess a tunable transverse dielectric response, we find remarkable variation in the launch angles of energy associated with the emission of leaky wave radiation. We write closed-form expressions for the energy transport velocity and corresponding radiation angle φ, defining the cone of radiation emission, as functions both of frequency and of material and geometrical parameters. Full wave simulations exemplify the broad range of directivity that can be achieved in these structures.

DOI: 10.1103/PhysRevB.84.075162 PACS number(s): 81.05.Xj, 42.25.Bs, 42.82.Et

I. INTRODUCTION

Metamaterials are composite structures engineered with subwavelength components, with the purpose of manipulating and directing electromagnetic (EM) radiation. Recently many practical applications have emerged, and structures related to cloaking, metamaterial perfect absorbers,[1] and chirality[2,3] have been fabricated. The desired EM response to the incident electric ($\boldsymbol{E}$) and magnetic ($\boldsymbol{H}$) fields typically involves tuning the permittivity ϵ and permeability μ in rather extraordinary ways. This includes double-negative-index media (negative real parts of both ϵ and μ), single-negative-index media (negative real part of ϵ *or* μ), matched impedance zero-index media[4,5] (real part of ϵ and μ is near zero), and epsilon-near-zero (ENZ) media (real part of ϵ is near zero). Scenarios involving ENZ media in particular have gained prominence lately as useful components to radiative systems over a broad range of the EM spectrum.[6–8] Composites containing an array of nanowires can behave as birefringent materials with ENZ properties along one direction.[9] Grating structures can also be designed to have properties akin to ENZ media.[10] In conjunction with ENZ developments, there have also been advances in infrared (IR) metamaterials, where thermal emitters,[11] optical switches,[12] and negative index metamaterials[2,13] have been fabricated. Due also in part to the broad possibilities in sensing technologies, this EM band is of considerable importance. Smaller scale metamaterial devices can also offer more complex and interesting scenarios, including tunable devices,[14] filters,[9] and nanoantennas.[15]

Anisotropy is an inextricable feature of metamaterials that plays a crucial role in their EM response. For instance, at optical and infrared frequencies, incorporating anisotropy into a thin planar (nonmagnetic) waveguide can result in behavior indicative of double-negative-index media.[16] Anisotropic metamaterial structures can now be created that contain elements that possess extreme electric and magnetic responses to an incident beam. The inclusion of naturally anisotropic materials that are also frequency dispersive (e.g., liquid crystals) allows additional control in beam direction. It has also been shown that metamaterial structures requiring anisotropic permittivity and permeability can be created using tapered waveguides.[17] By assimilating anisotropic metamaterial leaky wave structures within conventional radiative systems, the possibility exists to further control the emission characteristics.

Prompted by submicron experimental developments and the potential for unconventional beam manipulation, we investigate a planar anisotropic system with an ENZ response at near-IR frequencies along one of the principle axes (the longitudinal z direction). By tuning the electric and magnetic responses along the transverse axes, we demonstrate the ability to achieve remarkable emission control and directivity. When excited by a source, the direction of energy flow can be due to the propagation of localized surface waves. There can also exist leaky waves, whereby the energy radiatively "leaks" from the structure while attenuating longitudinally. Indeed, there can be a complex interplay between the different types of allowed modes, whether radiated or guided, or some other mechanism involving material absorption. Through a judicious choice of parameters, the admitted modes for the metamaterial can result in radiation launched within a narrow cone spanned by the outflow of energy flux.

Some of the earliest works involving conventional leaky wave systems reported narrow beamwidth antennas with prescribed radiation angles[18] and forward and backward leaky wave propagation in planar multilayered structures.[19] In the microwave regime, photonic crystals[11,20,21] and transmission lines can also can serve as leaky wave antennas.[22] More recently, a leaky wave metamaterial antenna exhibited broad side scanning at a single frequency.[22] The leaky wave characteristics have also been studied for grounded single- and double-negative metamaterial slabs.[23] Directive emission in the microwave regime was demonstrated for magnetic metamaterials in which one of the components of $\boldsymbol{\mu}$ is small.[24] Nonmagnetic uniaxially anisotropic slabs can also yield varied beam directivity.[25]

II. DISPERSION EQUATION

To begin our investigation, a harmonic time dependence, $\exp(-i\omega t)$, for the EM fields is assumed. The planar structure contains a central biaxial anisotropic metamaterial of width $2d$ sandwiched between the bulk superstrate and substrate, each of which can be anisotropic (see Fig. 1). In general, metamaterials

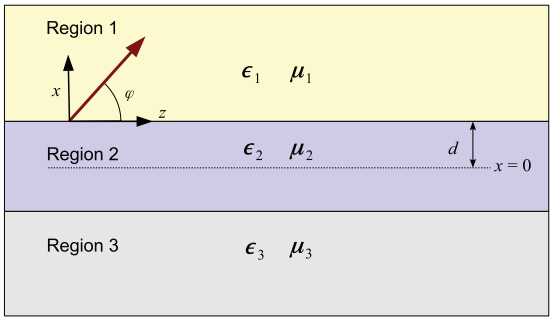

FIG. 1. (Color online) Schematic of the planar metamaterial structure. The central biaxial anisotropic metamaterial (region 2) is sandwiched between the superstrate (region 1) and substrate (region 3). All regions in general can have anisotropic permittivity and permeability tensors, $\boldsymbol{\epsilon}_i$ and $\boldsymbol{\mu}_i$, respectively [see Eqs. (1) and (2)]. The direction of energy outflow at the top surface of the metamaterial is depicted by the arrow in the xz plane and oriented at an angle φ relative to the z axis.

are resonant structures made from composite materials with inclusions or unit cells in principle much less than the operation wavelength. Depending on the geometry, strength of the resonance, and the material dissipation, the permittivity often cannot be described by the widely used Maxwell-Garnett approximation. More complicated expressions for the effective permittivity can be calculated by solving the full Maxwell equations. Regardless of the detailed nature of the permittivity, which may deviate from the conventional Drude type, the metamaterial can be considered homogeneous along any translationally invariant axis. In our case, the propagation distance of the leaky wave should be much longer than the unit cells in the longitudinal direction, while the thickness of the slab and the effective wavelength of the leaky wave should be much larger than the unit cells in the transverse direction.

We assume the material in each region is linear with a biaxial permittivity tensor,

$$\boldsymbol{\epsilon}_i = \epsilon_i^{xx}\hat{\boldsymbol{x}}\hat{\boldsymbol{x}} + \epsilon_i^{yy}\hat{\boldsymbol{y}}\hat{\boldsymbol{y}} + \epsilon_i^{zz}\hat{\boldsymbol{z}}\hat{\boldsymbol{z}}, \tag{1}$$

for $i = 1,2$, or 3. Similarly, the biaxial magnetic response is represented via

$$\boldsymbol{\mu}_i = \mu_i^{xx}\hat{\boldsymbol{x}}\hat{\boldsymbol{x}} + \mu_i^{yy}\hat{\boldsymbol{y}}\hat{\boldsymbol{y}} + \mu_i^{zz}\hat{\boldsymbol{z}}\hat{\boldsymbol{z}}. \tag{2}$$

The translational invariance in the y and z directions allows the magnetic field in the ith layer, $\boldsymbol{H}_i$, to be written [we consider transverse magnetic (TM) modes]:

$$\boldsymbol{H}_i(x,z) = \hat{\boldsymbol{y}}h_i^y(x)e^{i(\gamma z-\omega t)}, \tag{3}$$

and the electric field, $\boldsymbol{E}_i$, as

$$\boldsymbol{E}_i(x,z) = \left[\hat{\boldsymbol{x}}e_i^x(x) + \hat{\boldsymbol{z}}e_i^z(x)\right]e^{i(\gamma z-\omega t)}. \tag{4}$$

We define[26] the complex propagation constant, γ, in terms of the longitudinal phase, β, and attenuation α:

$$\gamma \equiv \beta + i\alpha. \tag{5}$$

We focus on leaky waves propagating in the positive x direction and possessing nonnegative β and α. Upon matching the tangential $\boldsymbol{E}$ and $\boldsymbol{H}$ fields at the boundaries, we arrive at the general dispersion equation that governs the allowed modes for this structure,

$$\epsilon_2^{zz}k_{\perp,2}\left(\epsilon_3^{zz}k_{\perp,1} + \epsilon_1^{zz}k_{\perp,3}\right) + \left[\left(\epsilon_2^{zz}\right)^2 k_{\perp,1}k_{\perp,3} - \epsilon_1^{zz}\epsilon_3^{zz}k_{\perp,2}^2\right]\tan(2dk_{\perp,2}) = 0, \tag{6}$$

where the transverse wave vector in the superstrate (referred to as region 1), $k_{\perp,1}$, is

$$k_{\perp,1} = \pm\sqrt{\epsilon_1^{zz}/\epsilon_1^{xx}(\beta^2-\alpha^2) - k_0^2\mu_1^{yy}\epsilon_1^{zz} + 2i\alpha\beta\epsilon_1^{zz}/\epsilon_1^{xx}}. \tag{7}$$

For convenience in the leaky wave analysis that follows, we have explicitly divided the argument of the square root in Eq. (7) into its real and imaginary parts. For the metamaterial region (region 2), we write

$$k_{\perp,2} = \pm\sqrt{k_0^2\mu_2^{yy}\epsilon_2^{zz} - \gamma^2\epsilon_2^{zz}/\epsilon_2^{xx}}, \tag{8}$$

and for the substrate (region 3), we write

$$k_{\perp,3} = \pm\sqrt{\gamma^2\epsilon_3^{zz}/\epsilon_3^{xx} - k_0^2\mu_3^{yy}\epsilon_3^{zz}}, \tag{9}$$

where $k_0 = \omega/c$. The choice of sign in regions 1 and 3 plays an important role in the determination of the physical nature of the type of mode solutions that will arise. The two roots associated with $k_{\perp,2}$, however, result in the same solutions to Eq. (6). The dispersion equation [Eq. (6)] can also be obtained from the poles of the reflection coefficient for a plane wave incident from above on the structure.

III. COMPLEX PROPAGATION CONSTANT

The factors of the $\boldsymbol{E}$ field in region 1 that depend on the transverse x direction are

$$e_1^z(x) = -\frac{ik_{\perp,1}}{k_0\epsilon_1^{zz}}H_1e^{-k_{\perp,1}(x-d)}, \tag{10}$$

$$e_1^x(x) = \frac{\gamma}{k_0\epsilon_1^{xx}}h_1^y, \tag{11}$$

where H_1 is a constant coefficient and the magnetic field factor, $h_1^y(x)$, is given by

$$h_1^y(x) = H_1e^{-k_{\perp,1}(x-d)}. \tag{12}$$

To disentangle the evanescent and leaky wave fields, we separate the wave vector $k_{\perp,1}$ into its real and imaginary parts:

$$k_{\perp,1} = \pm(q^- + iq^+), \tag{13}$$

with q^+ and q^- real. The wave vector $k_{\perp,1}$, and components $q^\pm$ are in general related, depending on $\mathrm{sgn}(\epsilon_1^{zz}\alpha\beta/\epsilon_1^{xx})$. For our $\exp(-i\omega t)$ time convention and for upward wave propagation (positive x direction), clearly we have $q^+q^- \geqslant 0$. It is also apparent that the parameter q^- represents the inverse length scale of wave increase along the transverse x direction. The combined evanescent and propagating modes are seen in the spatial behavior of the $\boldsymbol{H}$ field found in Eqs. (3) and (12):

$$\boldsymbol{H}_1(x,z) = \hat{\boldsymbol{y}}\mathcal{F}(x,z)e^{i[q^+(x-d)+\beta z-\omega t]}, \tag{14}$$

where the amplitude factor, $\mathcal{F}(x,z)$ is given by

$$\mathcal{F}(x,z) = H_1 e^{q^-(x-d)} e^{-\alpha z}. \tag{15}$$

Here we have expanded the complex $k_{\perp,1}$ and γ according to Eqs. (13) and (5), respectively. We see that the factor $\mathcal{F}(x,z)$ corresponds to wave amplitude increase in the transverse x direction while decaying in z, a hallmark of leaky waves. Although leaky wave modes are not localized, they can be excited by a point or line source which gives rise to limited regions of space of EM wave amplitude increase before eventually decaying. When explicitly decomposing $k_{\perp,1}$ into its real and imaginary parts, there is an intricate interdependence among γ, $\boldsymbol{\epsilon}_i$, and $\boldsymbol{\mu}_i$ (for $\alpha \neq 0$):

$$q^{\pm} = \frac{1}{\sqrt{2}}\left[\sqrt{\mathcal{A}^2 + \mathcal{B}^2} \mp \mathcal{A}\right]^{1/2}, \tag{16}$$

where

$$\mathcal{A} = \frac{\epsilon_1^{zz}}{\epsilon_1^{xx}}(\beta^2 - \alpha^2) - k_0^2 \mu_1^{yy} \epsilon_1^{zz}, \tag{17}$$

and

$$\mathcal{B} = 2\alpha\beta \frac{\epsilon_1^{zz}}{\epsilon_1^{xx}}. \tag{18}$$

It is further seen from Eq. (14) that q^+ and β are the relevant propagation factors in determining the behavior of leaky wave emission for our structure.

At this point, the surrounding media can have frequency dispersion in $\boldsymbol{\epsilon}_i$, and $\boldsymbol{\mu}_i$, while the anisotropic metamaterial region can be dispersive and absorptive. If we now take the limit $\epsilon_2^{zz} \to 0$ and consider a perfectly conducting ground plane, Eq. (6) can be solved analytically for the complex propagation constant (normalized by k_0),

$$\gamma^{\pm} = \frac{1}{\sqrt{2}} \frac{\sqrt{\left(\epsilon_2^{xx}\right)^2 + 8(k_0 d)^2 \epsilon_1^{xx}\epsilon_1^{zz}\epsilon_2^{xx}\mu_2^{yy} \pm \left|\epsilon_2^{xx}\right| \sqrt{\left(\epsilon_2^{xx}\right)^2 + (4k_0 d)^2 \epsilon_1^{zz}\epsilon_1^{xx}\left(\mu_2^{yy}\epsilon_2^{xx} - \mu_1^{yy}\epsilon_1^{xx}\right)}}}{2k_0 d\sqrt{\epsilon_1^{xx}\epsilon_1^{zz}}}. \tag{19}$$

The two possible roots correspond to distinct dispersion branches (seen below). There are, in all, four solutions, $\gamma^{\pm}$ and $-\gamma^{\pm}$. The geometrical and material dependence contained in Eq. (19) determines the entire spectrum of the leaky wave modes that may exist in our system. Depending on the media in regions 1 and 2, represented by the tensors $\boldsymbol{\epsilon}_1$, $\boldsymbol{\mu}_1$, $\boldsymbol{\epsilon}_2$, and $\boldsymbol{\mu}_2$, as well as the frequency ω and thickness parameter d, the leaky wave attenuation factor α (the imaginary component of γ^+) can have nontrivial behavior.

IV. ENERGY TRANSPORT VELOCITY

There are numerous quantities one can study in order to effectively characterize leaky wave emission. One physically meaningful quantity is the energy transport velocity, $\boldsymbol{v}_T$, which is the velocity at which EM energy is transported through a medium.[27,28] It is intuitively expressed as the ratio of the time-averaged Poynting vector, $\boldsymbol{S}_{\text{avg}}$, to the energy density, U:

$$\boldsymbol{v}_T \equiv \frac{\boldsymbol{S}_{\text{avg}}}{U}. \tag{20}$$

Properly accounting for frequency dispersion that may be present, we can thus express the energy transport velocity above the structure as

$$\boldsymbol{v}_T = \frac{c/(8\pi)\text{Re}[\boldsymbol{E}_1 \times \boldsymbol{H}_1^*]}{1/(16\pi)\left[\boldsymbol{E}_1^\dagger \cdot \frac{d(\omega\boldsymbol{\epsilon}_1)}{d\omega}\boldsymbol{E}_1 + \boldsymbol{H}_1^\dagger \cdot \frac{d(\omega\boldsymbol{\mu}_1)}{d\omega}\boldsymbol{H}_1\right]}, \tag{21}$$

where the conventional definition[29] of U has been extended to include anisotropy. Inserting the calculated EM fields and assuming no dispersion in the superstrate, we find

$$\boldsymbol{v}_T = \omega \frac{\left(\epsilon_1^{xx} q^+ \hat{\boldsymbol{x}} + \epsilon_1^{zz}\beta\hat{\boldsymbol{z}}\right)}{\epsilon_1^{zz}\beta^2 + \epsilon_1^{xx}(q^+)^2}. \tag{22}$$

The corresponding angle of energy outflow, φ, is determined by the direction that $\boldsymbol{v}_T$ makes, with the positive z axis (see Fig. 1),

$$\varphi = \arctan\left(\frac{\epsilon_1^{xx} q^+}{\epsilon_1^{zz}\beta}\right), \tag{23}$$

which holds in the case of loss and frequency dispersion in the metamaterial. We will study φ as a function of ϵ_2^{xx}, d, and frequency. The energy outflow direction will be shown in some cases to vary from normal ($\varphi = \pi/2$) to broadside ($\varphi = 0$). For the cases studied in this paper, φ was also found to be weakly dependent on absorption in the metamaterial (arising solely from the component ϵ_2^{xx}). It is evident that Eq. (23) satisfies $\varphi \to 0$ as $\alpha \to 0$, corresponding to the disappearance of leaky waves and the possible emergence of guided waves. In this limit, $\boldsymbol{v}_T = \hat{z}\omega/\beta$, which corresponds to the expected velocity at which plane wave fronts travel along the $+z$ direction. There is also angular symmetry, where $\varphi(\epsilon_2^{xx}) \to \varphi(-\epsilon_2^{xx})$, when $\mu_2^{yy} \to -\mu_2^{yy}$. For high refractive index media (ϵ_2^{xx} or $\mu_2^{yy} \to \infty$), we moreover recover the expected result that φ tends toward broadside ($\varphi = 0$).

V. RESULTS

To determine the properties of leaky waves for our anisotropic structure, we study the normalized complex propagation constant, γ^+, from Eq. (19). We consider, in addition to a perfectly conducting ground plane, the upper region (region 1) to be in vacuum (so that $\epsilon_1^{zz} = \epsilon_1^{xx} = \mu_1^{yy} = 1$). In Figs. 2(a) and 2(c), 3D views depict the normalized β (real part of γ^+) and normalized α (imaginary part of γ^+) as functions of the transverse dielectric response ϵ_2^{xx} and thickness parameter d (recall the width equals $2d$). In Figs. 2(b) and 2(d), corresponding 2D slices depict the normalized β and

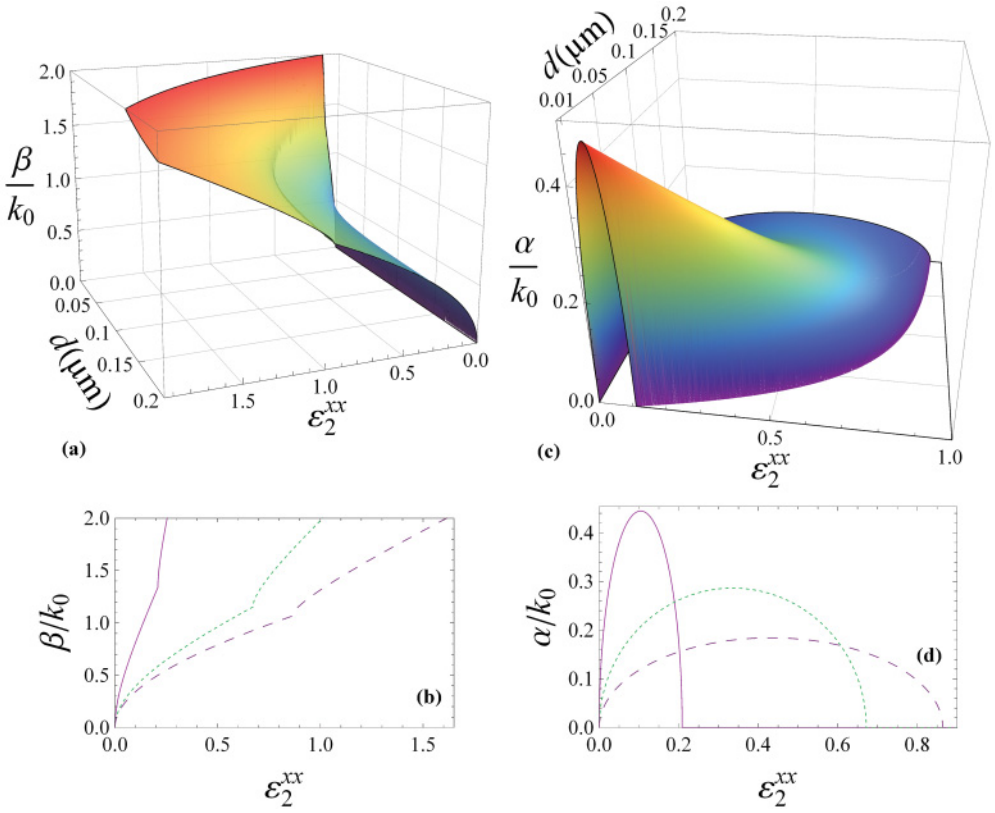

FIG. 2. (Color online) The real (β) and imaginary (α) parts of the complex propagation constant γ^+, normalized by the vacuum wave vector k_0 at $f = 280$ THz ($\mu_2^{yy} = 1$). Panels (a) and (c) are three-dimensional (3D) global views depicting α and β as functions of ϵ_2^{xx} and the thickness parameter d. Panels (b) and (d) represent the normalized β and α, respectively, as functions of ϵ_2^{xx} and for $d = 0.01$ μm (solid curve), $d = 0.05$ μm (dotted curve), and $d = 0.1$ μm (dashed curve).

α as functions of ϵ_2^{xx} for various fixed widths. Only the positive root, γ^+, is shown, corresponding to the leaky wave cases of interest, where $\alpha \geqslant 0$. The slight kinks in the curves observed in Fig. 2(b) correlate with the vanishing of α at the same ϵ_2^{xx}, observed in Fig. 2(d), and also indicate the points where the γ^- solutions would emerge (when $\alpha < 0$). The values of ϵ_2^{xx} corresponding to these crossover points is given below, in Eq. (27). Both panels on the left clearly demonstrate that β changes more rapidly as a function of ϵ_2^{xx} for smaller widths. Indeed, for subwavelength widths ($k_0 d \ll 1$), and to lowest order, the real part of the propagation constant varies linearly in ϵ_2^{xx} and inversely in d,

$$\frac{\beta}{k_0} \approx \frac{\epsilon_2^{xx}}{2k_0 d\sqrt{\epsilon_1^{xx}\epsilon_1^{zz}}}. \tag{24}$$

If we now fix the structure width and expand Eq. (19) to lowest order in ϵ_2^{xx}, corresponding to an approximately isotropic ENZ slab (where $\epsilon_2^{zz} = 0$ and ϵ_2^{xx} is near zero), we find

$$\frac{\beta}{k_0} \approx \sqrt{\frac{\epsilon_2^{xx}}{2}}[\sqrt{1 + 1/(2k_0 d)^2} + 1]^{1/2} \tag{25}$$

and

$$\frac{\alpha}{k_0} \approx \sqrt{\frac{\epsilon_2^{xx}}{2}}[\sqrt{1 + 1/(2k_0 d)^2} - 1]^{1/2}, \tag{26}$$

where $\mu_2^{yy} = 1$. It is evident from these expressions and Fig. 2 that both β and α tend to zero as $\epsilon_2^{xx} \to 0$ (long wavelength limit), and we will see below that the direction of energy outflow rapidly approaches normal to the interface. It is also interesting that the important parameter α characterizing leaky waves rapidly increases from zero at $\epsilon_2^{xx} = 0$ and peaks at differing values, depending on the width of the emitting structure [Figs. 2(c) and (d)], until eventually returning to zero at the two points,

$$\epsilon_2^{xx} = 4[-2(k_0 d)^2 \pm \sqrt{(k_0 d)^2 + 4(k_0 d)^4}]. \tag{27}$$

This illustrates that α is spread over a greater range of ϵ_2^{xx} for larger widths, but as previously discussed in conjunction with Fig. 2, α simultaneously suffers a dramatic reduction. For small d/λ, the extremum of Eq. (19) reveals that the strength of the α peaks, $\alpha_{\max}$, are approximately given by

$$\alpha_{\max} \approx \tfrac{1}{2} \pm k_0 d. \tag{28}$$

Next we investigate the emission angle φ, which defines the direction $\boldsymbol{v}_T$ makes relative to the surface of the metamaterial structure. We first calculate the complex γ^+ from Eq. (19) and then extract α and β, which are inserted into Eq. (16) to determine q^+. We can then determine φ via Eq. (23) as a function of the relevant geometrical and material parameters. In Fig. 3(a), the behavior of φ is shown as a function of ϵ_2^{xx} for nonmagnetic media ($\mu_2^{yy} = 1$), while Fig. 3(b) corresponds to a metamaterial with vanishing μ_2^{yy}, representative of a type of matched impedance.[5] The four curves in Figs. 3(a)

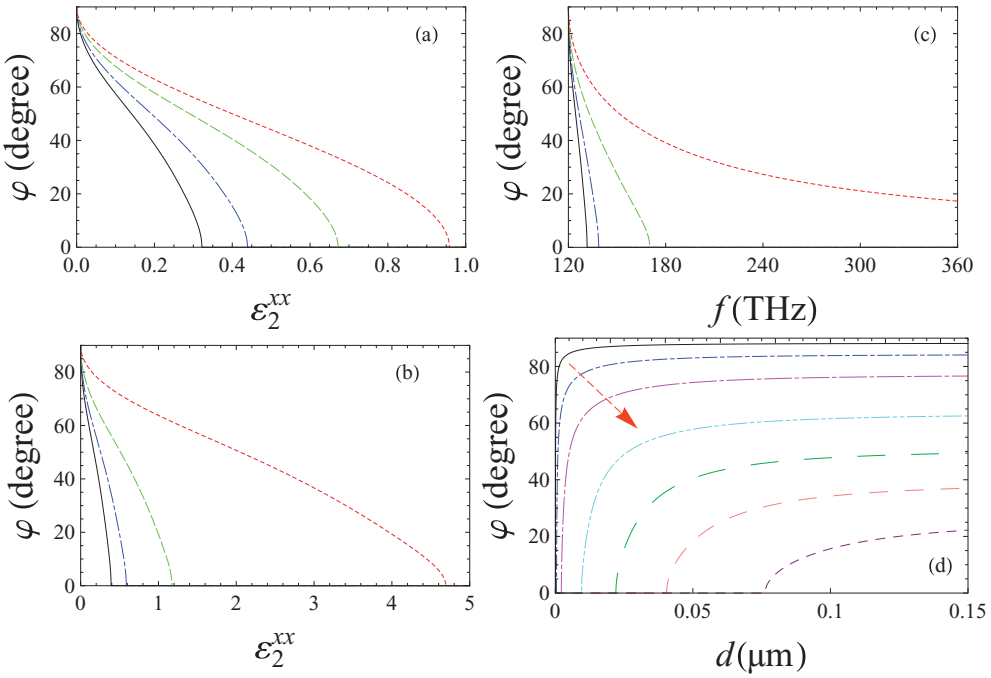

FIG. 3. (Color online) Leaky wave launch angle φ as a function of ϵ_2^{xx} [(a) and (b)] for $d = 1/5\ \mu$m (dotted red curves) and successively smaller values of d equaling 1/20,1/40, and 1/60 (in μm). In (a) $\mu_2^{yy} = 1$, and in (b) $\mu_2^{yy} = 0$. In (c) the emission angle is shown as a function of frequency for the same thicknesses in (a) and (b), and also for $\mu_2^{yy} = 1$. In (d) the effects of geometrical variation are presented for $\epsilon_2^{xx} = 0.001,0.01,0.05,0.2,0.4,0.6$, and 0.8 ($\mu_2^{yy} = 1$). The arrow depicts the progression of curves with successively larger values of ϵ_2^{xx}. Each panel [except (c)] corresponds to the frequency in Fig. 2.

and 3(b) correspond to different widths, identified in the caption. We see that for $\epsilon_2^{xx} \to 0$, we recover the isotropic result of nearly normal emission ($\varphi \approx 90^o$), discussed and demonstrated in the millimeter regime.[6] This behavior can be understood in our system, at least qualitatively, from a geometrical optics perspective and a generalization of Snell's law for bianisotropic media.[30] When the magnetic response vanishes [Fig. 3 (b)], the emission angle becomes symmetric with respect to ϵ_2^{xx}, declining from normal ($\varphi = \pi/2$) at $\epsilon_2^{xx} = 0$ to broadside ($\varphi = 0$) when

$$\epsilon_2^{xx} = \pm 4k_0 d. \tag{29}$$

Thus thinner widths result in more rapid beam variation as a function of ϵ_2^{xx}.

In Fig. 3(c) we show how the emission angle varies as a function of frequency f with the transverse response obeying a Drude form,

$$\epsilon_2^{xx} = 1 - \frac{\omega_p^2}{\omega^2 + i\Gamma\omega}. \tag{30}$$

We set $\omega_p = (2\pi)120$ THz, and for simplicity and to isolate leaky wave effects, we also set $\Gamma = 0$. We consider a frequency ranging from 120 to 360 THz, corresponding to ϵ_2^{xx} varying from 0 to approximately 0.89, respectively. With increasing frequency (and hence increasing ϵ_2^{xx}), we observe trends similar to those found in the previous figures, where a larger dielectric response pulls the beam toward the metamaterial.

In Fig. 3(d), a geometrical study illustrates how the emission angle varies with thickness: For $\epsilon_2^{xx}\mu_2^{yy} < 1$, the emission angle rises abruptly with increased d, before leveling off at

$$\varphi = \arctan\left(\sqrt{\frac{1}{\epsilon_2^{xx}\mu_2^{yy}} - 1}\right). \tag{31}$$

Physically, as the slab increases in size, the complex propagation constant becomes purely real,

$$\gamma \to \sqrt{\epsilon_2^{xx}\mu_2^{yy}}, \tag{32}$$

and consequently

$$q^+ \to \sqrt{1 - \epsilon_2^{xx}\mu_2^{yy}}. \tag{33}$$

This is consistent with what was discussed previously involving the depletion of α with d; for thick ENZ slabs, leaky wave radiation is replaced by conventional propagating modes. For fixed ϵ_2^{xx}, there is also a critical thickness d^* below which no leaky waves are emitted, which by Eq. (19) is

$$d^* = \frac{\epsilon_2^{xx}}{4k_0\sqrt{1 - \epsilon_2^{xx}\mu_2^{yy}}}. \tag{34}$$

We now take our planar anisotropic structure and introduce a magnetic line source[25] operating at a frequency of 280 THz. The resultant EM fields are calculated using a commercial finite element software package.[31] In Fig. 4, the normalized $|\boldsymbol{H}|$ is shown (the arrows represent energy outflow) with the source directed along the y axis (we consider only TM mode excitations) and centrally positioned at the feed of the

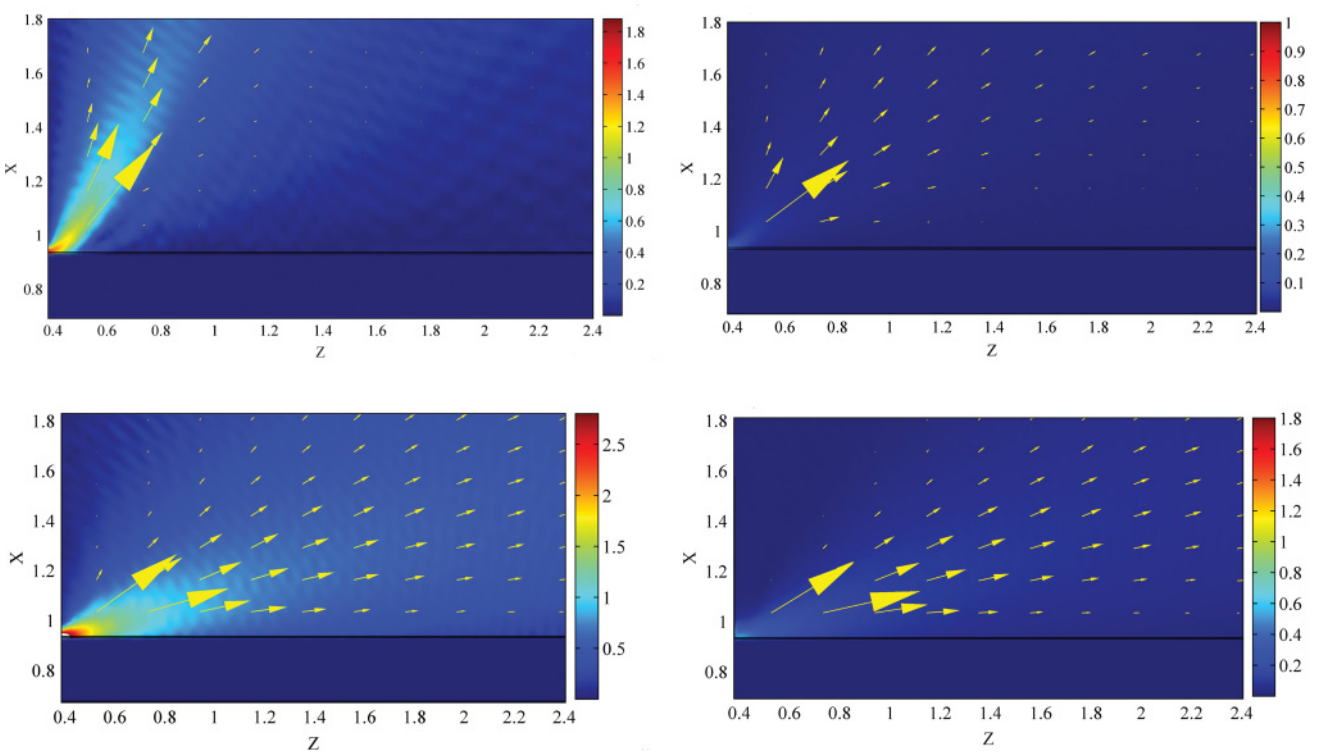

FIG. 4. (Color online) Normalized magnetic field profiles illustrating broad angular variation in beam emission. The arrows depict the Poynting vectors throughout the spatial domain, normalized by their respective fields. The set of four panels illustrates the EM response for an anisotropic ENZ ($\epsilon_2^{zz} \approx 0$) structure without absorption (left set) and with a moderate amount of absorption, corresponding to an imaginary component of ϵ_2^{xx} equal to 0.3 (right set). The top and bottom rows of panels correspond to the real part of ϵ_2^{xx} equaling 0.05 and 0.66 respectively. The metamaterial is subwavelength ($2d = 1/10\ \mu$m) and nonmagnetic ($\mu_2^{yy} = 1$). Coordinates are given in units of ($\times 10$) μm.

metamaterial. We take a slab width of $1/10\ \mu$m and set $\epsilon_2^{zz} \approx 0$ for the ENZ axis. To illustrate the range of directivity we consider four representative values of ϵ_2^{xx}: two cases with loss (right panels) and two without loss (left panels). We find qualitative agreement with the results of Fig. 3, in which the leaky wave energy outflow can span a broad range as ϵ_2^{xx} is varied. The figures also demonstrate [and as stated below Eq. (23)], minimal deviation in φ with moderate amounts of absorption.

VI. CONCLUSIONS

In conclusion, we have presented a transcendental dispersion equation for the allowed modes of a general three-region planar system exhibiting biaxial anisotropy. We then solved the dispersion equation for the case of a biaxial metamaterial in vacuum possessing a vanishing dielectric response along the longitudinal z axis and backed by a perfectly conducting metal. We solved the dispersion equation analytically for the complex propagation constant and extracted the relevant α and β factors. Both α and β were studied as functions of thickness of the metamaterial slab and the transverse component to the permittivity tensor ϵ_2^{xx}. We found a variety of leaky wave solutions that can exist over a range of ϵ_2^{xx}, smaller than unity, and which depend on the thickness parameter d. We calculated the energy transport velocity $\boldsymbol{v}_T$ and demonstrated that by appropriately tuning ϵ_2^{xx}, the corresponding direction of energy outflow can span a broad range of emission angles φ. We also calculated the minimum thickness of the metamaterial structure which could support leaky waves.

Although fabricating nanoscale metamaterials with low absorption currently faces challenges, continual progress has been made in systems involving fishnet structures,[32] electromagnetically induced transparency,[33] and gain-assisted materials.[34] Other viable candidates might incorporate plasmonic and doped semiconductor materials.[35] Recent nanofabrication techniques involving focused ion beam milling[36] and nanodeposition[9] also offer further progress toward the practical creation of low-loss metamaterial nanostructures.

ACKNOWLEDGMENT

K.H. is supported in part by ONR and a grant of HPC resources as part of the DOD HPCMP.

[1]X. Liu, T. Starr, A. F. Starr, and W. J. Padilla, Phys. Rev. Lett. **104**, 207403 (2010).

[2]S. Zhang, Y. S. Park, J. Li, X. Lu, W. Zhang, and X. Zhang, Phys. Rev. Lett. **102**, 023901 (2009).

[3]C. Menzel, C. Helgert, C. Rockstuhl, E. B. Kley, A. Tunnermann, T. Pertsch, and F. Lederer. Phys. Rev. Lett. **104**, 253902 (2010).
[4]R. W. Ziolkowski, Phys. Rev. E **70**, 046608 (2004).
[5]V. C. Nguyen, L. Chen, and K. Halterman, Phys. Rev. Lett. **105**, 233908 (2010).
[6]S. Enoch, G. Tayeb, P. Sabouroux, N. Guerin, and P. Vincent, Phys. Rev. Lett. **89**, 213902 (2002).
[7]M. Silveirinha and N. Engheta, Phys. Rev. Lett. **97**, 157403 (2006).
[8]A. Alù *et al*., Phys. Rev. B **75**, 155410 (2007).
[9]L. V. Alekseyev *et al*., Appl. Phys. Lett. **97**, 131107 (2010).
[10]V. Mocella *et al*., Opt. Express **18**, 25068 (2010).
[11]M. Laroche, R. Carminati, and J. J. Greffet, Phys. Rev. Lett. **96**, 123903 (2006).
[12]N.-H. Shen, M. Massaouti, M. Gokkavas, J. M. Manceau, E. Ozbay, M. Kafesaki, T. Koschny, S. Tzortzakis, and C. M. Soukoulis, Phys. Rev. Lett. **106**, 037403 (2011).
[13]S. Zhang, W. Fan, N. C. Panoiu, K. J. Malloy, R. M. Osgood, and S. R. J. Brueck, Phys. Rev. Lett. **95**, 137404 (2005).
[14]N.-H. Shen, M. Massaouti, M. Gokkavas, J. M. Manceau, E. Ozbay, M. Kafesaki, and T. Koschny, Phys. Rev. Lett. **106**, 037403 (2011).
[15]X-X. Liu and A. Alù, Phys. Rev. B **82**, 144305 (2010).
[16]V. A. Podolskiy and E. E. Narimanov, Phys. Rev. B **71**, 201101(R) (2005).
[17]I. I. Smolyaninov, V. N. Smolyaninova, A. V. Kildishev, and V. M. Shalaev, Phys. Rev. Lett. **102**, 213901 (2009).
[18]R. E. Collin and F. J. Zucker, *Antenna Theory, Part II* (McGraw-Hill, New York, 1969).
[19]T. Tamir and F. Y. Kou, IEEE J. Quantum Electr. **22**, 544 (1986).
[20]E. Colak *et al*., Opt. Express **17**, 9879 (2009).
[21]A. Micco, V. Galdi, F. Capolino, A. DellaVilla, V. Pierro, S. Enoch, and G. Tayeb, Phys. Rev. B **79**, 075110 (2009).
[22]S. Lim, IEEE Trans. Microwave Theory Tech. **52**, 2678 (2004).
[23]P. Baccarelli *et al*., IEEE Trans. Microwave Theory Tech. **53**, 32 (2005).
[24]Y. Yuan, L. Shen, L. Ran, T. Jiang, J. Huangfu, and J. A. Kong, Phys. Rev. A **77**, 053821 (2008).
[25]H. Liu and K. J. Webb, Phys. Rev. B **81**, 201404(R) (2010).
[26]P. L. Overfelt, K. Halterman, S. Feng, and D. R. Bowling, J. Appl. Phys. **108**, 124310 (2010).
[27]R. Loudon, J. Phys. A **3**, 233 (1970).
[28]R. Ruppin, Phys. Lett. A **299**, 309 (2002).
[29]L. D. Landau, E. M. Lifshitz, and L. P. Pitaevskii, *Electrodynamics of Continuous Media*, 2nd ed. (Butterworth-Heinemann, Oxford, 1984).
[30]T. M. Grzegorczyk *et al*., IEEE Trans. Microwave Theory Tech. **53**, 1443 (2005).
[31]COMSOL MULTIPHYSICS [http://www.comsol.com].
[32]C. Garcia-Meca, J. Hurtado, J. Marti, A. Martinez, W. Dickson, and A. V. Zayats, Phys. Rev. Lett. **106**, 067402 (2011).
[33]P. Tassin, L. Zhang, T. Koschny, E. N. Economou, and C. M. Soukoulis, Phys. Rev. Lett. **102**, 053901 (2009).
[34]S. Xiao *et al*., Nature (London) **466**, 735 (2010).
[35]A. Boltasseva and H. A. Atwater, Science **331**, 290 (2011).
[36]S. Burgos *et al*., Nat. Mat. **9**, 407 (2010).